Available online at www.sciencedirect.com
ScienceDirect
International Journal of Heat and Fluid Flow 29 (2008) 495–503
International Journal of HEAT AND FLUID FLOW
www.elsevier.com/locate/ijhff

Boundary layer receptivity measurements on compliant surfaces

Jui-Che Huang, Mark W. Johnson *

Department of Engineering, University of Liverpool, Brownlow Hill, Liverpool L69 3GH, UK

Received 2 June 2007; received in revised form 24 September 2007; accepted 26 November 2007
Available online 9 January 2008

Abstract

This paper describes receptivity measurements in a pre-transitional boundary layer flowing over either a rigid or a compliant surface. Fluctuating velocities and frequency spectra were determined on one rigid and nine compliant surfaces. The results showed that the near wall receptivity grows linearly with Re_θ. An empirical correlation of the gain frequency spectrum for a rigid wall was also established. For the compliant surfaces, the near wall gain is increased markedly near the leading edge of the plate due to the amplification of high and mid-frequencies. These frequencies are dissipated though as the flow progresses over the compliant surface such that the receptivity is lower on all the compliant surfaces than on the rigid surface at the trailing edge. An empirical correlation for the ratio of the gains on compliant and rigid surfaces in terms of the compliant surface coefficient $\zeta^2/E\rho_{CS}L^2$ and Re_θ was established. This correlation indicates that compliant surfaces can suppress receptivity by up to 25% for a $Re_\theta = 400$.

Keywords: Compliant surface; Boundary layer transition; Boundary layer receptivity

1. Introduction

Saving energy has always had economic benefits, but has recently also become important in reducing global warming. Engineers in the transport industries in particular are therefore eager to reduce aerodynamic drag over their vehicles to reduce fuel consumption. One way of achieving this is to suppress the laminar to turbulent transition of the boundary layers, as a turbulent boundary layer can result in more than double the drag of a laminar one. Many techniques have been proposed to achieve this suppression such as compliant surfaces, riblets, transverse vibration, and boundary layer suction. Compliant surfaces have the advantages of being passive, simple, inexpensive and easy to retrofit to existing vehicles, but as yet have shown only modest performance.

During the last few decades, considerable research has been done on transition delay and turbulent drag reduction through the use of compliant surfaces. Most of this work has been concerned with turbulent flow or natural transition, where the freestream turbulence level is low (<1%). It has been shown (Willis, 1986) that for low freestream turbulence the Tollmien–Schlichting (T–S) waves, which cause transition, can be suppressed by using compliant surfaces. For a turbulent flow over a compliant surface, Choi et al. (1997) has also shown that modest drag reduction can be achieved using rubber compliant surfaces on cylindrical bodies in water flow. Fluctuating pressures generated by unsteadiness in the flow cause the compliant surface to move and hence fluctuation energy is transferred from the flow to the surface. If the natural frequency for the surface is such that significant energy is removed from the flow and the surface material has sufficient damping to dissipate this energy, then the fluctuation energy in the flow is reduced resulting in delayed transition and turbulent drag reduction. However, a compliant surface with the wrong properties can increase rather than decrease the fluctuation energy in the boundary layer.

For flows exposed to high freestream turbulence levels ($Tu > 1\%$), T–S waves do not appear and transition occurs through a bypass mechanism. In practice the flow mechanisms associated with both T–S waves and bypass

* Corresponding author. Tel.: +44 151 794 4818; fax: +44 151 794 4848.
E-mail address: m.w.johnson@liv.ac.uk (M.W. Johnson).

0142-727X/$ - see front matter © 2007 Elsevier Inc. All rights reserved.
doi:10.1016/j.ijheatfluidflow.2007.11.004

Nomenclature

$e(\Omega_x)$	energy spectral density in the near wall region ($y/\delta < 0.2$)	u	air velocity
$E(\Omega_x)$	energy spectral density in the freestream	u_{rms}	rms fluctuating air velocity
E	Young's modulus for compliant surface material	U	freestream air velocity
f	streamwise fluctuation frequency	U_{rms}	rms fluctuating freestream velocity
F_c	frequency at which the gain is 0.5 G_0	x	streamwise distance
G_0	low frequency gain	y	wall normal distance
Gain	ratio of local and freestream turbulence levels	α_C	compliant surface material property coefficient ($\zeta^2/E\rho_{CS}L^2$)
Gain(Ω_x)	gain at a particular streamwise frequency	δ	boundary layer thickness
$Gain_{NW}$	near wall gain	λ	Pohlhausen pressure gradient parameter
$Gain_{ratio}$	ratio between compliant and rigid surface gain	ν	kinematic viscosity
k_i	coefficients used in Eq. (7) ($i = 1, 6$)	θ	boundary layer momentum thickness
L	thickness of compliant surface (4 mm)	ρ_{CS}	density of compliant surface material (1000 kg/m^3)
R^2	correlation coefficient	Ω_x	dimensionless streamwise frequency ($2\pi f\delta/U$)
Re_θ	momentum thickness Reynolds number ($U\theta/\nu$)	ζ	damping coefficient for compliant surface material
S	gradient of the gain attenuation		
Tu	freestream turbulence level		

transition are present in all boundary layer flows, but the freestream turbulence level determines which will dominate the transition process. It is important therefore that a compliant surface is capable of suppressing both T–S and bypass flow mechanisms. Huang and Johnson (2007) have studied bypass transition on nine compliant surfaces and have shown that a modest (3%) delay in transition can be achieved for a freestream turbulence level of 1.8% if the compliant surface material properties are optimised. Receptivity is the mechanism through which fluctuations in the boundary layer near wall region are induced by the freestream turbulence. It therefore follows that if a compliant surface is able to reduce receptivity then a delay in transition and a reduction in turbulent drag will result.

The objective of the current work is to extend the previous work of Huang and Johnson (2007) to determine how compliant surfaces influence the boundary layer receptivity process which leads to bypass transition.

2. Experimental method

The experiments were conducted in the 1050 mm long by 310 mm wide by 155 mm high outlet section of a blower wind tunnel (see Fig. 1). The test plate, which has a 6:1 elliptic leading edge and is of 15 mm thickness was located at mid-height within the test section. Morkovin (1969) stated that for transition to occur through a bypass rather than a T–S mode, the freestream turbulence level Tu must exceed 1%. For this reason, the tunnel freestream turbulence level was increased from the natural level of about 0.3 to 1.8% at the leading edge using a grid (square mesh of 1.2 mm diameter wires 12 mm apart) placed 432 mm (36 mesh pitches) upstream of the leading edge. The

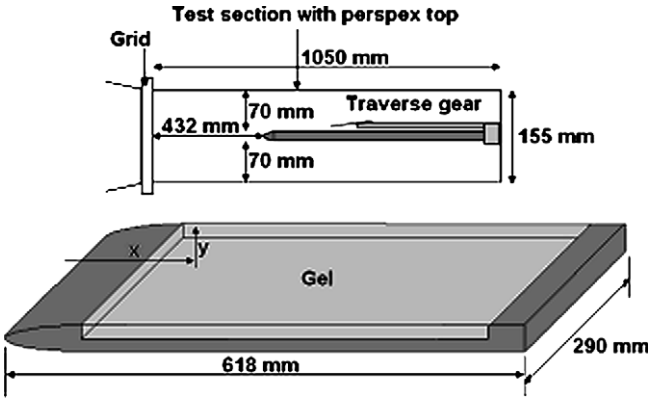

Fig. 1. Experimental setup.

integral length scale for the freestream turbulence at the leading edge was estimated as 4.6 mm using the Roach (1987) correlation. In contrast to Huang and Johnson's (2007) work, where transitional boundary layers were studied, in the current work, a lower tunnel speed of 6.5 m/s was used throughout such that the boundary layer remained laminar along the full length of the plate.

The experimental arrangement was designed such that the environments for the rigid and compliant surface measurements were identical. To this end the symmetrical aluminium test plate had a 4 mm deep × 618 mm long cavity machined in one surface 25 mm from the leading edge, in which the compliant surface material was placed. The plate could be removed from the tunnel and inverted such that the measurements on both rigid and compliant surfaces were always performed on the upper surface. The compliant surfaces were manufactured from gelatine covered by a 10 μm protective PVC film. An accurately measured quantity of hot water and gelatine mix was poured

into the plate cavity and allowed to set prior to being covered with the protective film. This ensured that the surface was flat with no surface curvature due to surface curvature at the edges. Measurements of the surface height were made at 10 streamwise stations and were found to differ by less than 0.2 mm. The compliant surface properties were altered by changing the quantity of gelatine in the mix. Full details of the manufacture of the compliant surfaces are given in Huang (2006) and Huang and Johnson (2007). The properties of the compliant surfaces used in the present study are given in Table 1. Huang and Johnson (2007) introduced a dimensionless quantity $\zeta^2/E\rho_{CS}L^2$ (hereafter called the compliant surface coefficient α_C) which represents the material properties of the compliant surface. These properties are the damping factor (ζ), the Young's modulus (E), the coating density (ρ_{CS}) and the coating thickness (L). Details of how these parameters were measured are given in Huang and Johnson (2007). This compliant surface coefficient is analogous to the damping coefficient used in dynamics to characterise the ability of a mass, spring, damper system to attenuate vibrations. In the current study, the compliant surface coefficient therefore characterises the ability of a compliant surface to dissipate the fluid's fluctuation energy.

The measurements were made using a DISA M system anemometer connected to a single DISA 55P15 boundary layer probe. The probe was traversed using a computer controlled traverse mechanism which was placed over the compliant surface on a cantilever fixed at the trailing edge of the plate. Boundary layer traverses were performed at four streamwise stations at $x = 112$, 195, 277 and 340 mm from the leading edge. Each traverse consisted of at least 30 y location measurements within the boundary layer and a further 10 locations outside the boundary layer up to at least twice the boundary layer thickness, where the unsteady velocity had reached its freestream value. A sample of 45 s duration with a sample rate of 20 kHz was used at each location.

The streamwise pressure gradient along the plate was slightly favourable (Pohlhausen pressure gradient parameter λ of approximately two), due to the blockage caused by the boundary layer within the constant cross sectional area of the passage above the plate.

Table 1
The properties of the compliant surfaces used in the experiments

E (N/m^2)	ζ (Ns/m^2)	$\zeta^2/E\rho_{CS}L^2$
900	7.17	3.49
2000	14.18	6.13
3600	10.87	2.00
3800	12.83	2.65
4000	5.44	0.45
4000	10.26	1.61
5300	23.52	6.37
8100	25.61	4.94
8700	26.39	4.89

3. Results

3.1. Rigid surface measurements

Johnson and Ercan (1999) considered the receptivity of boundary layers to freestream disturbances. The receptivity of the boundary layer can be quantified by considering the gain, which is the ratio of the near wall turbulence level (the output) to the freestream turbulence level at the same streamwise position (the input), i.e.

$$\text{Gain} = \frac{u_{rms}}{u} \Big/ \frac{U_{rms}}{U} \tag{1}$$

The gain profiles across the boundary layer at each of the four measurement stations at a tunnel speed of 6.5 m/s are shown in Fig. 2. The highest gain values occur adjacent to the wall, but the gain is approximately constant in the near wall region which is defined here by the shaded region in Fig. 2, i.e. y/δ below 0.2.

Fig. 2 also shows how the near wall gain increases as the boundary layer develops. The nature of this development can be seen more clearly in Fig. 3 which shows the boundary layer growth for a variety of freestream velocities. These results show that the near wall gain grows linearly with Re_θ in the pre-transitional boundary layer. Brandt et al. (2004) simulated bypass transition using DNS and observed that the fluctuations in the pre-transitional boundary layer were dominated by streak like structures. They found that the ratio between the energies of these fluctuations and those in the freestream was proportional to streamwise distance, i.e. (u_{rms}/U_{rms}) is proportional to Re_θ. Johnson and Ercan (1999) came to a similar conclusion from their transition experiments on flat plates. The best fit straight line shown in Fig. 3 is

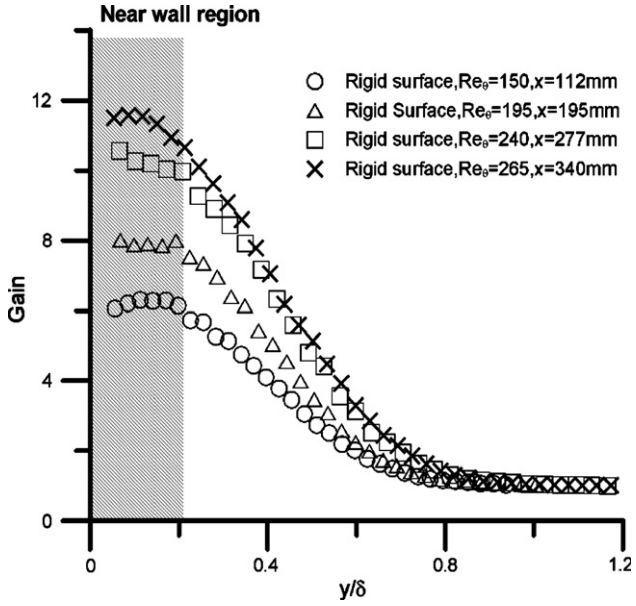

Fig. 2. Gain profile across boundary layer.

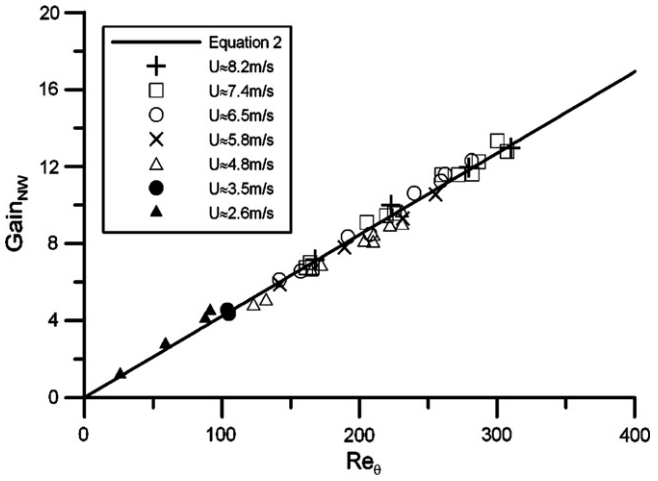

Fig. 3. Near wall gain for the rigid wall.

$$\mathrm{Gain}_{\mathrm{NW}} = 0.0423 Re_\theta \tag{2}$$

This empirical correlation will be used later as a benchmark for comparison with results from the compliant surfaces.

3.2. Spectral results

Spectral analysis of the near wall and freestream velocity signals enables the identification of the frequencies to which the boundary layer is most receptive. The near wall gain for a particular frequency is defined as

$$\mathrm{Gain}(\Omega_x) = \left(\frac{e(\Omega_x)}{E(\Omega_x)}\right)^{\frac{1}{2}} \frac{U}{u} \tag{3}$$

where $e(\Omega_x)$ and $E(\Omega_x)$ are the power spectral densities in the near wall region and in the freestream, respectively. It therefore follows that the overall gain is given by

$$\mathrm{Gain}_{\mathrm{NW}} = \frac{\left(\int_0^\infty e(\Omega_x)\mathrm{d}\Omega_x\right)^{\frac{1}{2}}}{\left(\int_0^\infty E(\Omega_x)\mathrm{d}\Omega_x\right)^{\frac{1}{2}}} \frac{U}{u} \tag{4}$$

The freestream and near wall spectra for a boundary layer where $Re_\theta = 150$ are shown in Fig. 4a with the resulting gain spectrum. For high frequencies, the gain has a low amplitude. This is because the smallest vortices decay rapidly and even more rapidly within the shear layer close to the wall. In contrast, at low frequencies high gain values are measured and hence demonstrate that it is these low frequencies which dominate the receptivity process. The same observation was made by Jacobs and Durbin (2001) for their DNS results. Theoretical work by Johnson (2002) suggests that these amplified low frequencies are associated with the streamwise streaky structures observed in pre-transitional boundary layers by, for example, Matsubara and Alfredsson (2001).

3.2.1. Empirical correlation of gain spectrum

The gain spectrum in Fig. 4b can be represented by an equation of the form

$$\mathrm{Gain}(\Omega_x) = \frac{G_0}{1 + \left(\frac{\Omega_x}{F_c}\right)^S} \tag{5}$$

This equation has three coefficients. G_0 is the low frequency gain and determines the gain for the low frequency plateau in the spectra. It is this part of the spectra which contributes most to the overall gain and hence to the receptivity process. F_c is the frequency at which the low frequency gain is reduced by 50%, i.e. the -3 dB point. Finally S is the attenuation slope which determines the rate of decrease in the high frequency gain. These three parameters were computed for each boundary layer profile using a non-linear least squares data fitting procedure and are plotted in Fig. 5. Correlation equations were then fitted to these three curves. The empirical correlations for G_0 and F_c give excellent fits ($R^2 > 0.90$), whereas the fit for the slope S is less reliable ($R^2 = 0.60$). As already discussed though, S is of secondary importance as it is the extent and magnitude of the low frequency gain which is dominant in determining the receptivity. The overall empirical correlation for the spectral near wall gain is therefore

$$\mathrm{Gain}(\Omega_x) = \frac{2.42 \times 10^{-4} Re_\theta^2 + 7.80 \times 10^{-2} Re_\theta}{1 + \left(\Omega_x (0.0553 Re_\theta + 4.59)\right)^{2.15}} \tag{6}$$

and is shown in Fig. 6.

Fig. 6 shows that this equation gives a reliable representation of the gain spectra for the range of Re_θ values obtained for the laminar boundary layer considered in the present work. Fig. 7 shows the variation in gain over the full range of Re_θ and Ω_x.

3.2.2. Critical frequency band

Although it is the lowest frequencies which are most strongly amplified and which dominate the receptivity process, they do not dominate the transition process. Johnson (2001) has suggested that transient separation of the laminar boundary layer is the mechanism by which turbulent spots are induced. It follows therefore that if any fluctuation frequency reaches the critical amplitude necessary to produce transient separation, then spots will be induced, but the higher the frequency the greater the spot production rate. The frequencies resulting in the highest spot production are therefore the highest frequencies which have a gain close to the maximum of G_0, i.e. of the order of F_c. These frequencies correspond approximately with the wavelengths of 15–20δ identified by Mayle et al. (1997, 1998) as the most significant in the transition process. It is therefore these disturbances in the mid-frequency range which play the most important role for boundary layer transition.

The significance of these frequencies can be more correctly represented by plotting the 'gain times frequency' values as shown in Fig. 8. The frequency range can then be split into three bands using the -5 db points either side of the peak.

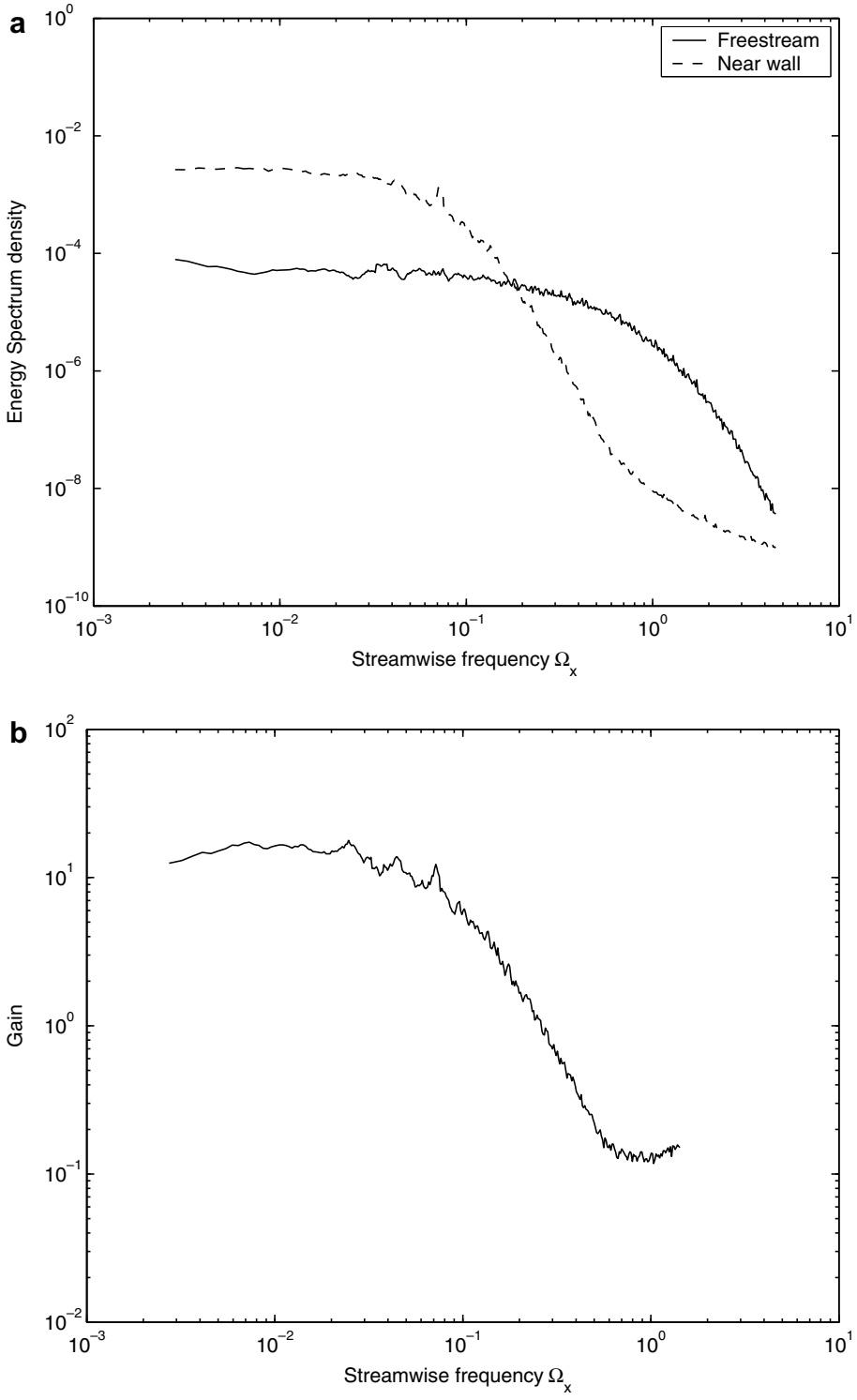

Fig. 4. (a) Freestream and near wall energy spectrum, (b) gain spectrum for $Re_\theta = 155$.

3.3. Compliant surface measurements

Huang and Johnson (2007) showed that there were no significant differences between the boundary layer profiles and growth rates on the rigid surface and the nine compliant surfaces listed in Table 1. They concluded that the influence of the compliant surfaces on the mean flow quantities for the pre-transitional boundary layer is negligible.

3.3.1. Boundary layer receptivity for the compliant surfaces

The boundary layer receptivity was determined for each of the nine compliant surfaces at each of the four

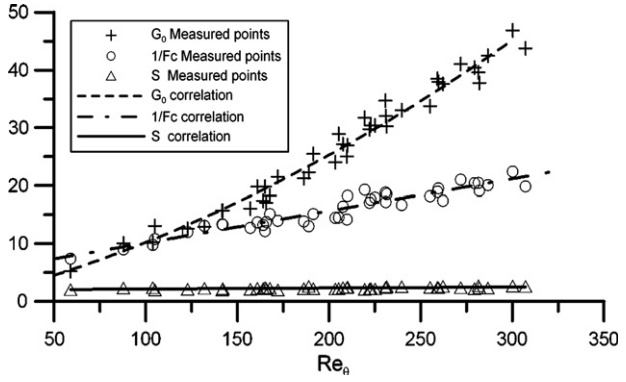

Fig. 5. Correlations of gain curve parameters.

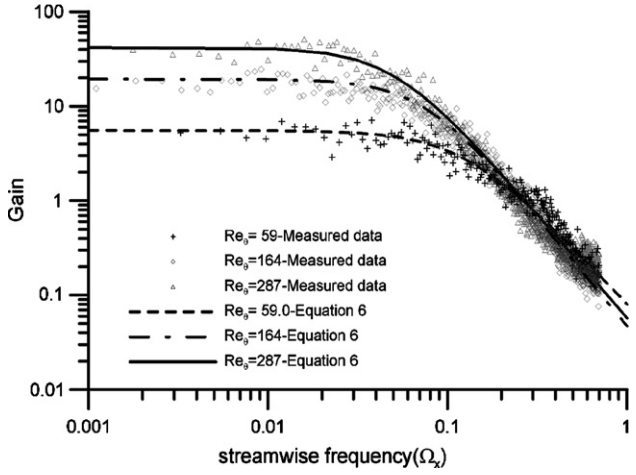

Fig. 6. Measured gain spectra.

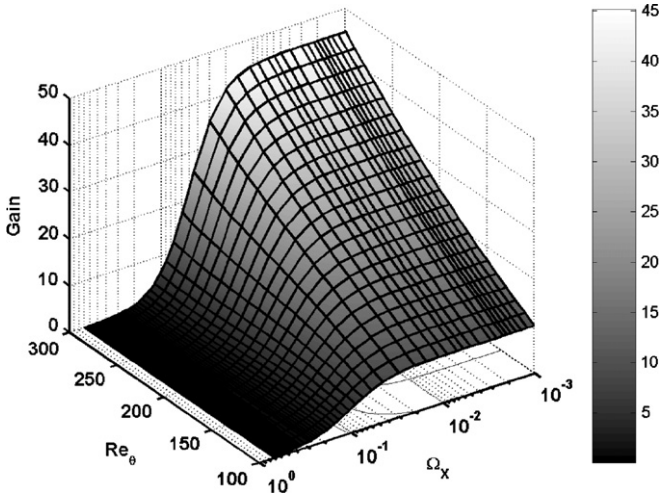

Fig. 7. Gain correlation.

measurement stations ($x = 112$, 195, 277 and 340 mm) with a fixed freestream velocity $U = 6.5$ m/s at the leading edge.

Fig. 9 shows the compliant surface gains (non-dimensionalised with the rigid plate gain at the same location).

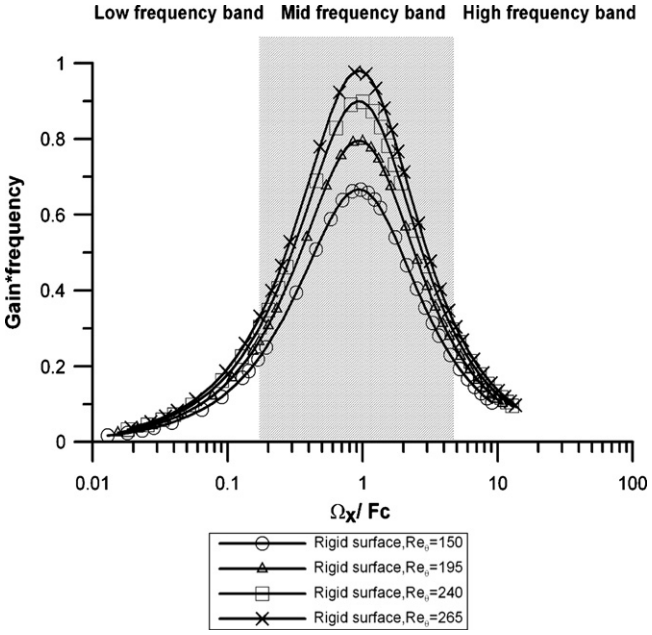

Fig. 8. Frequency bands.

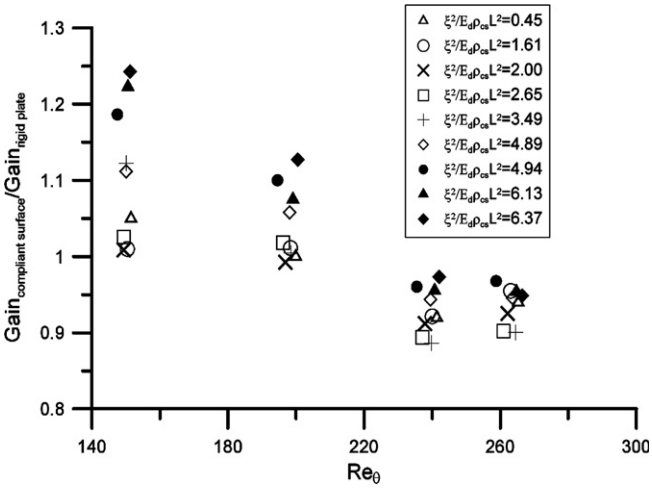

Fig. 9. Gain ratio evolution with Re_θ.

This figure shows that all the compliant surfaces result in increased boundary layer receptivity at the first two measurement stations with a maximum increase of 24% in near wall boundary layer receptivity at the first measurement location. The receptivity also increases approximately in proportion with the compliant surface coefficient α_C. However, the boundary layer fluctuations are progressively suppressed, in comparison to the rigid surface, as the flow moves downstream, such that the receptivity is lower than for the rigid surface for all the compliant surfaces at both the third and fourth measurement stations. The $\alpha_C = 3.49$ compliant surface is the most successful in reducing the receptivity with reductions of 11.3% and 10.0% for the last two stations where Re_θ equals 240 and 265, respectively.

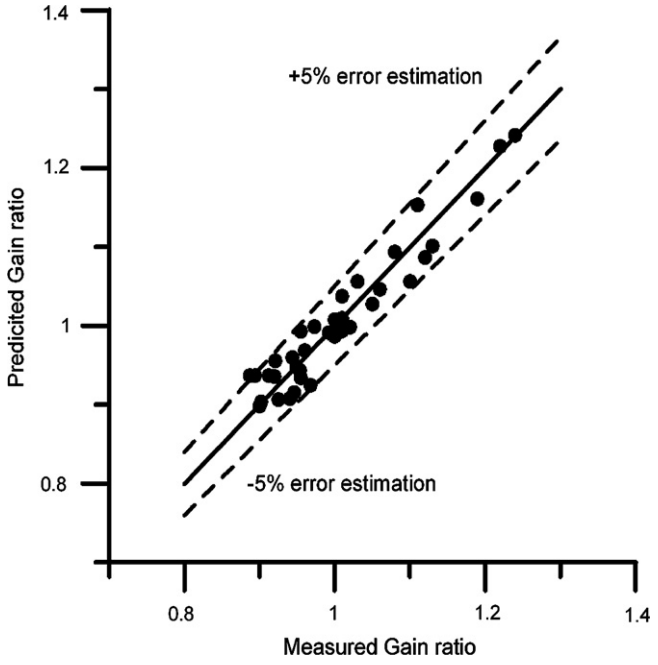

Fig. 10. Comparison of gain ratio measurements with empirical equation.

3.3.2. Receptivity performance of compliant surfaces

A least squares surface fit to the data in Fig. 11a was achieved by considering a wide range of different equation forms (a total of about 30,000). The equation with the lowest rms error was

$$\mathrm{Gain}_{\mathrm{ratio}} = (k_1 + k_2\alpha_c + k_3\alpha_c^2) + (k_4 + k_5\alpha_c)/Re_\theta + k_6/Re_\theta^2 \quad (7)$$

where $k_1 = 0.529$, $k_2 = -0.0790$, $k_3 = 0.00499$, $k_4 = 161$, $k_5 = 12.7$ and $k_6 = -1340$.

The correlation coefficient (R^2) for this equation was 0.92 and the maximum discrepancy between the measured data and the fitted surface was 5% as shown in Fig. 10. Eq. (7) is therefore reasonably reliable in predicting the gain ratio for any zero pressure gradient boundary layer flowing over any compliant surface with a α_C within the range studied in the present work. It is therefore of interest to extrapolate this surface to higher values of Re_θ to see how successful these compliant surfaces might be in reducing receptivity for lower freestream turbulence levels where Re_θ will be lower at transition inception.

The extrapolation in Fig. 11b indicates that a maximum receptivity suppression of 25% can be achieved for an $Re_\theta = 400$ and an α_C of between 4 and 5. This suggests that for a freestream turbulence level of 1%, where transition, Mayle (1991), would occur at a Re_θ of 400 on a rigid plate, transition could be delayed until $Re_\theta = 500$ as the $\mathrm{Gain}_{\mathrm{NW}}$ is proportional to Re_θ or an approximately 50% increase in streamwise distance, as Re_θ is proportional to $\sqrt{Re_x}$.

3.4. Gain spectra for compliant surface boundary layers

The results just discussed show that compliant surfaces are capable of reducing receptivity, but it is also of interest to know which frequencies they are most successful in suppressing. The gain times frequency spectra at the four streamwise stations and for four of the compliant surfaces are shown together with the rigid surface results in Fig. 12. All the data presented here is for pre-transitional boundary layers and so the measured intermittency is zero throughout. The shaded area depicts the mid-frequency band for the rigid wall results from the gain Re_θ relationship (Eq. (6)).

The compliant surfaces have most influence on the high and mid-frequency bands at the first two stations particularly when α_C is greater than four. This increase in boundary layer receptivity results in earlier spot generation in the flow and hence earlier transition as observed by Huang and Johnson (2007). As the flow moves downstream, the energy in the high and mid-frequency bands begins to dissipate and by the final measurement station the peak in the gain times frequency curve is reduced for all the compliant surfaces. The maximum reduction occurs for the $\alpha_C = 2.65$ and 3.49 surfaces. When $\alpha_C < 2$, the mid-frequencies only dissipate slowly over the compliant surface, whereas, for high α_C the energy dissipation is much more rapid. The highest α_C surfaces would therefore be the most successful

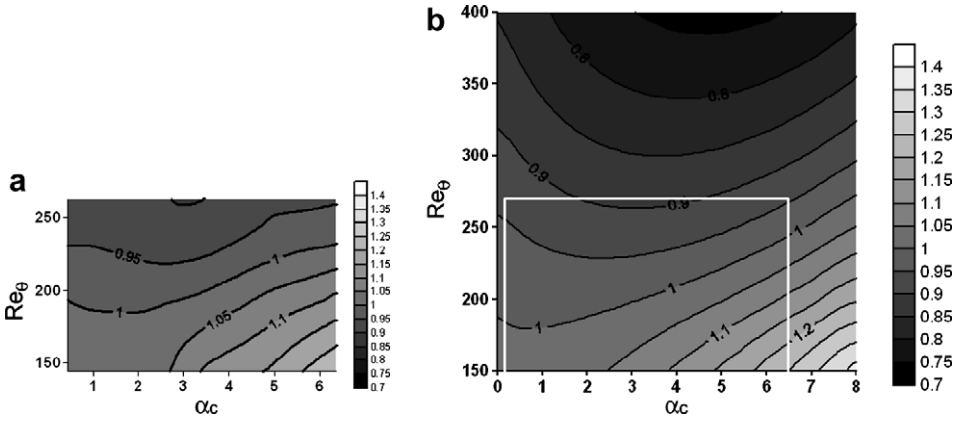

Fig. 11. (a) Measured gain ratio, (b) gain ratio from empirical equation.

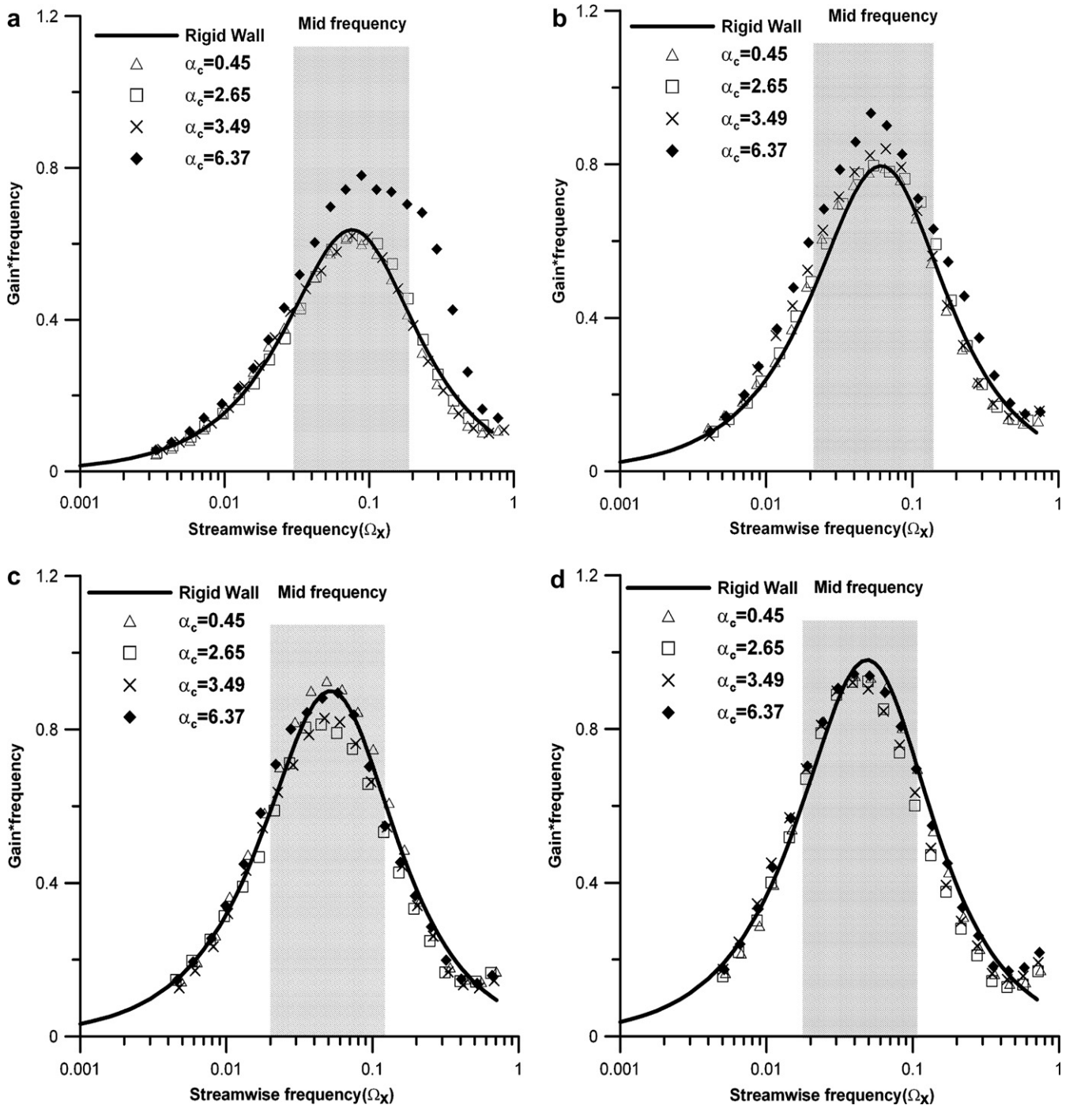

Fig. 12. Spectra of gain times frequency for compliant surfaces. (a) $Re_\theta = 150$, $x = 112$ mm, (b) $Re_\theta = 195$, $x = 195$ mm, (c) $Re_\theta = 240$, $x = 277$ mm, (d) $Re_\theta = 265$, $x = 340$ mm.

if it were not for the high levels of fluctuation induced at the leading edge.

4. Conclusion

The boundary layer receptivity for the flow over rigid and compliant surfaces with a moderate freestream turbulence level (1.1–1.8%) were investigated. The main conclusions of the work are that:

1. An empirical correlation for gain spectra for the full laminar range of Re_θ for a zero pressure gradient boundary layer over a rigid surface has been established.
2. The lowest frequency fluctuations dominate the receptivity process, but it is the mid-frequency range fluctuations which dominate transition. The gain times frequency spectra is therefore a good indicator of the effectiveness of a compliant surface to suppress transition.

3. The ratio between compliant and rigid surface gains can be represented by an empirical function of the compliant surface coefficient $\zeta^2/E\rho_{CS}L^2$ and Re_θ.
4. The current results suggest that compliant surfaces, of the type investigated here, can achieve a receptivity reduction of 25% for a Re_θ of 400.
5. On a compliant surface, mid-range frequencies within the boundary layer are amplified at the leading edge particularly for high values of $\zeta^2/E\rho_{CS}L^2$. However, as the flow travels over the compliant surface these frequencies are more effectively dissipated which leads to a lower receptivity than for a rigid surface at the trailing edge.

References

Brandt, L., Schlatter, P., Henningson, D.S., 2004. Transition in boundary layers subject to free-stream turbulence. J. Fluid Mech. 517, 167–198.

Choi, K.S., Yang, X., Clayton, B.R., Glover, E.J., Atlar, M., Semenov, B.N., Kulik, V.M., 1997. Turbulent drag reduction using compliant surfaces. Proc. R. Soc. London 453, 2229–2240.

Huang, J.C., 2006. Boundary layer receptivity of flow over compliant surfaces. PhD Thesis. Department of Engineering, University of Liverpool.

Huang, J.C., Johnson, M.W., 2007. Boundary layer receptivity of flow over compliant surfaces. Exp. Fluids 42 (May), 711–718.

Jacobs, R.G., Durbin, P.A., 2001. Simulations of bypass transition. J. Fluid Mech. 428, 185–212.

Johnson, M.W., 2001. On the flow structure in a turbulent spot. Int. J. Heat Fluid Flow 22, 409–416.

Johnson, M.W., 2002. Predicting transition without empiricism or DNS. ASME J. Turbomach. 124, 665–669.

Johnson, M.W., Ercan, A.H., 1999. A physical model for bypass transition. Int. J. Heat Fluid Flow 202, 95–104.

Mayle, R.E., 1991. The role of laminar-turbulent transition in gas turbine engines. ASME J. Turbomach. 113, 509–537.

Mayle, R.E., Schultz, A., 1997. The path to predicting bypass transition. ASME J. Turbomach. 1193, 405–411.

Mayle, R.E., Dullenkopf, K., Schultz, A., 1998. The turbulence that matters. ASME J. Turbomach. 120, 402–409.

Morkovin, M.V., 1969. On the many faces of transition. In: Wells, C.S. (Ed.), Viscous Drag Reduction. Plenum, NY.

Matsubara, M., Alfredsson, P.H., 2001. Disturbance growth in boundary layers subjected to free-stream turbulence. J. Fluid Mech. 430, 149–168.

Roach, P.E., 1987. The generation of nearly isotropic turbulence by means of grids. Int. J. Heat Fluid Flow 8, 82–92.

Willis, G.J.K., 1986. Hydrodynamic stability of boundary layer over Kramer type compliant surfaces. PhD Thesis. University of Exeter.